V European Conference on Computational Fluid Dynamics
ECCOMAS CFD 2010
J. C. F. Pereira and A. Sequeira (Eds)
Lisbon, Portugal, 14–17 June 2010

THE TELFONA PATHFINDER MODEL, A SECOND LOOK

Thomas Streit[*], Géza Schrauf[†], Itham Salah El Din[††], Ubaldo Cella[§], Uwe Fey[**], Yasuhiro Egami[**]

[*]DLR, D-38108 Braunschweig, Germany
e-mail: th.streit@dlr.de

[†]Airbus, D-28199 Bremen, Germany
e-mail: geza.schrauf@airbus.com

[††]ONERA Chalais-Meudon, 92320 France
e-mail: itham.Salah_el_din@onera.fr

[§]Piaggio Aero Industries ,80078 Pozzuoli (NA), Italy
e-mail: ucella@piaggioaero.it

[**]DLR, D-37073 Göttingen, Germany
e-mail: uwe.fey@dlr.de, y.egami@coe.mech.nagoya-u.ac.jp

Key words: CFD, Natural Laminar Flow, Cryogenic Temperature Sensitive Paint, Stability Analysis, Laminar-Turbulent Transition

Abstract. *Within the European Project Telfona the Pathfinder Model was designed, analyzed numerically, constructed and tested with the aim to obtain the capability of laminar flow testing of the European Transonic Wind Tunnel (ETW). The model was designed for natural laminar flow (NLF) for transonic flow conditions with high Reynolds number. Pre-test numerical analysis results demonstrated that the Pathfinder wing pressure distribution was adequate to provide calibration test points. The ETW tests provided pressure distribution data and transition position obtained from images using the Cryogenic Temperature Sensitive Paint Method (cryroTSP). The evaluation of this data with several transition prediction tools was used to establish the transition N-factor values for ETW. In this work, after test CFD solutions are obtained using numerical Navier-Stokes solutions. Stability analysis is performed using the local stability 2-N factor method. In the first part of this work, it is shown that for the range of flow conditions tested, the Pathfinder wing pressure distribution is sufficiently insensitive to different parameters like span, transition position and turbulence model. In the second part, it is shown that for selected flow conditions a good agreement is obtained between stability analysis based on experimental data and numerical data. In the third part the numerical analysis and experimental data are used complementarily*

1 INTRODUCTION

The Telfona Pathfinder model was designed, analyzed numerically, constructed and tested for evaluating the possibility of laminar flow testing of the European Transonic Wind Tunnel (ETW). It was designed for allowing natural laminar flow (NLF) at transonic, high Reynolds number flow conditions. Telfona (Testing for Laminar Flow and New Aircraft) is a European Research Project led by Airbus. The design and pre-test stability analysis for the Pathfinder wing has been described in [1]. The experimental data provided pressure distributions which are required to perform stability analysis. Transition locations were determined using Cryogenic Temperature Sensitive Paint Method (cryroTSP) [2]. Details of the wind tunnel tests are given in [3,4]. The experimental data from the first and second Pathfinder ETW tests was processed and linear stability was performed by Airbus [5]. The linear stability results show that data were sufficient to obtain critical ETW N-factors for cases with either predominant Tollmien Schlichting (TS) N-factors N_{TS} or for predominant crossflow (CF) N-factors N_{CF}. The processed pressure distributions were then sent to the other Telfona partners DLR, CIRA, FOI, ONERA in order to perform stability analysis using several different methods. The analysis of this processed experimental data using local stability theory and database methods was summarized in [3,4]. In the present work, post-test CFD solutions have been obtained by Airbus/DLR, ONERA and Piaggio Aero. Numerical results are compared to the experimental ones and are used to complement the stability analysis.

The specifications of the Pathfinder wing are described in section 2. Section 3 describes the numerical methods used for CFD and stability analysis. Results are given in section 4. The result section has three parts. In the first part, CFD solutions are used to show the properties of the Pathfinder model. In the second part, numerical results for the pressure distribution and N-factors are compared to corresponding data obtained from the experiments. In the third part, numerical solutions are obtained for the third ETW Pathfinder test campaign. No pressure distribution data exist for this test campaign. Using pressure distributions obtained numerically, and the TSP images from the ETW test, further cases were selected to complement the calibration of the critical ETW N-factors. Conclusions are given in section 5.

2 SPECIFICATIONS OF PATHFINDER WING

The Telfona Pathfinder model is a wing body configuration (see Fig.1). The wing leading edge has a 18° sweep, span s and chord c are limited by wind tunnel size, i.e. $s < 1.8$m, $c < 0.25$m. Due to its small taper the Pathfinder wing planform looks like a rectangular swept wing. For the design it was required that pressure distribution of spanwise sections should result in a linear variation of the amplification N-factor as function of chord position. Furthermore it was required that for the design point parallel isobars are obtained for a region which at least extends from 30% to 70% span, with transition occurring between 30% and 50% percent chord. It was designed for expected N-factors ranges: $5< N_{CF}<8$, $6 <N_{TS}< 10$ (local stability, incompressible) [1]. The fuselage with belly fairing geometry is taken from an existing ETW model. Design point is M=0.78, Re=20 mill., C_L=0.216. The relevant test flow conditions for the test section are: Ma=0.78±0.02, Re= 15 to 23 millions, T_{Tot}= 117°K to ambient temperature, C_L= 0.1 to 0.5 Side slip β=0° and -4. The model has TSP patches on upper and lower wing surfaces (see Fig. 1). Pressure taps are located on diagonal sections which are

roughly located at normalized semispan positions η=0.33, 0.67 (Fig.2). Both the port and starboard wing are equipped with pressure taps.

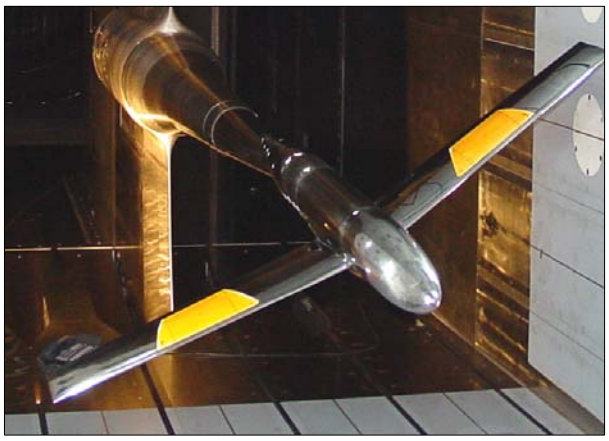

Figure 1: TELFONA PATHFINDER Model in ETW wind tunnel test section.

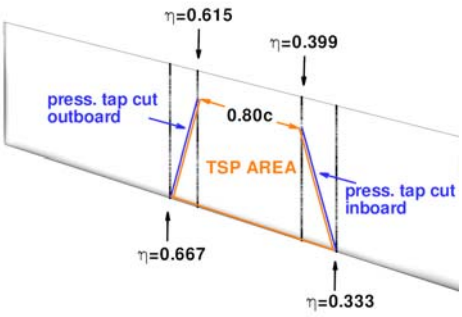

Figure 2: Position of TSP patches and pressure tap sections.

3 MESH GENERATION, NUMERICAL METHODS

Meshes generated in this work are based on a CAD geometry obtained with the pre-test design geometry [1]. It is the same CAD geometry which was used to construct the wind tunnel model. CFD solutions are presented by DLR/Airbus, ONERA, and Piaggio Aero.

DLR uses a hybrid unstructured mesh generated by Airbus. It has 14.77 mill. points, with 3.93 mill. tetrahedra, and 27.94 mill. prism. RANS solutions are obtained using the DLR-TAU-code [6]. For turbulence modelling the algebraic Spalart Allmaras model is used as well as the 2 equation SST model. Solutions are obtained with a full turbulent layer and fixed transition. Piaggio Aero generated a structured mesh with 15 millions hexahedral cells. The wing surface has 101 sections spanwise, each with 451 points in chord direction. RANS solutions are obtained using the CFD++ code [7]. The q-ω SST turbulence model is used for fully turbulent solutions.

Linear stability theory is performed using LILO[8], which is embedded in the STABTOOL program. In STABTOOL the three programs: PREPCP, COCO and LILO are used sequentially. PREPCP pre-processes the input pressure distributions in order to prepare it for boundary layer calculation. COCO performs boundary layer calculation for the stability analysis, which is performed by LILO. LILO uses a N_{TS}/N_{CF} method, in which N_{TS} is obtained by using the constant ψ strategy at frequencies covering the complete range of unstable waves, and N_{CF} is obtained by considering only stationary instabilities, using either the constant wavelength strategy or the constant spanwise wavenumber β^* strategy. In this approach, the N-factors are computed using incompressible equations. Used stability analysis assumes an adiabatic wall temperature.

Slightly different tools are used at ONERA. Mean flow was computed using the structured code elsA [9], in RANS mode and with the Spalart-Allamaras turbulence model. Then, post-processing of computed or measured pressure distributions allows the preparation of input data for the transition prediction. For this activity, ONERA uses both a database method inserted into the 3D boundary layer code 3C3D [10], or linear local stability theory for compressible flows with the CASTET code [11]. Compressible N_{TS}/N_{CF} or the envelope method are classically used.

4 RESULTS

Stability analysis and CFD results are given in this section. In the first subsection the CFD solutions are analyzed regarding the specification of the Pathfinder model and its usefulness for stability analysis. In the second subsection numerical results are compared to experimental data from ETW Phase I and II. In the third subsection numerical results are obtained for ETW Phase III cases.

4.1 Properties of the Pathfinder model

TAU-RANS solutions for two flow condition are given in Fig. 3 to illustrate the parallel isobar concept of the Pathfinder wing. Shown are pressure distributions for sections with η=0.33 and η=0.67. Flow conditions are M=0.78, Re=20 mill. and C_L=0.208 and C_L=0.320. The solution at C_L=0.208 is compared to the original design solution given in [1], which showed perfect parallel isobars within these span sections. Here for the lower side there is a good agreement with the original target, whereas for the upper part differences are obtained in the sensitive transonic region, especially at the shock position. After excluding some of the possible causes for these differences it was

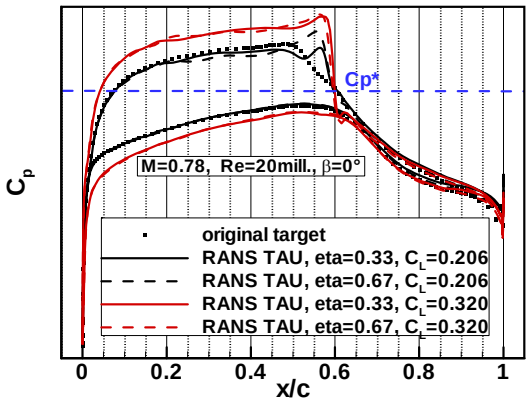

Figure 3. Pressure distributions for TAU-RANS solution illustrating isobar concept

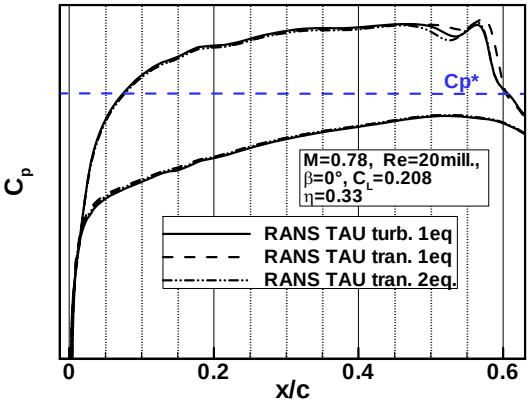

Figure 4. Sensitivity of solution to selected turbulence model and transition position.

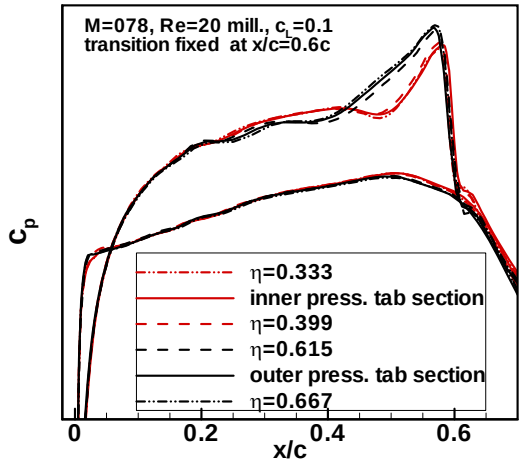

Fig 5. Spanwise variation of pressure distribution. Flow condition: M=0.78, Re=20 mill., C_L=0.1.

concluded that they may be attributed to small geometry oscillations between the definition sections, which originated in the CAD construction process and to a smaller extent to mesh refinement differences in the solution. For the higher incidence parallel isobars are also obtained at the upper side.

Figure 4 demonstrates that the Pathfinder pressure distribution is relatively independent of the used turbulence models and of either fixing transition or not. In order to see the differences more clearly the shown part of the pressure distribution is amplified in a region from the nose up to the pressure minimum. The turbulent boundary layer was modelled with the 1 equation SA model or with the 2-equation SST model. Transition position was fixed at x/c=0.6.

Since the solutions show insensitivity of Cp to transition position and turbulence model it was decided to obtain the rest of the TAU solutions within this work (if not indicated) by fixing transition at x/c=0.6 and using the 2-eq. SST model .

Stability analysis in this work is based on pressure distribution input. The pressure distributions at a constant span section are used to compute longitudinal and transversal boundary layer data using the conical assumption. The latter assumes that in spanwise direction pressure distribution does not vary along constant normalized chord positions. For the Pathfinder model this requirement is satisfied also for off design flow conditions as shown in Figure 5. For this case on the lower side the parallel isobar concept is also achieved.

In Fig. 6 a comparison of stability analysis is shown for RANS Cp-distributions solutions obtained with the TAU and the CFD++ code. Stability analysis was performed using the LILO code. Flow conditions are M=0.78, Re=18 million, C_L=0.1. There is a good agreement in the pressure distribution. Effective sweep angle was obtained from the CFD solutions. Results for N_{CF}-factor are closer together than N_{TS}-factors.

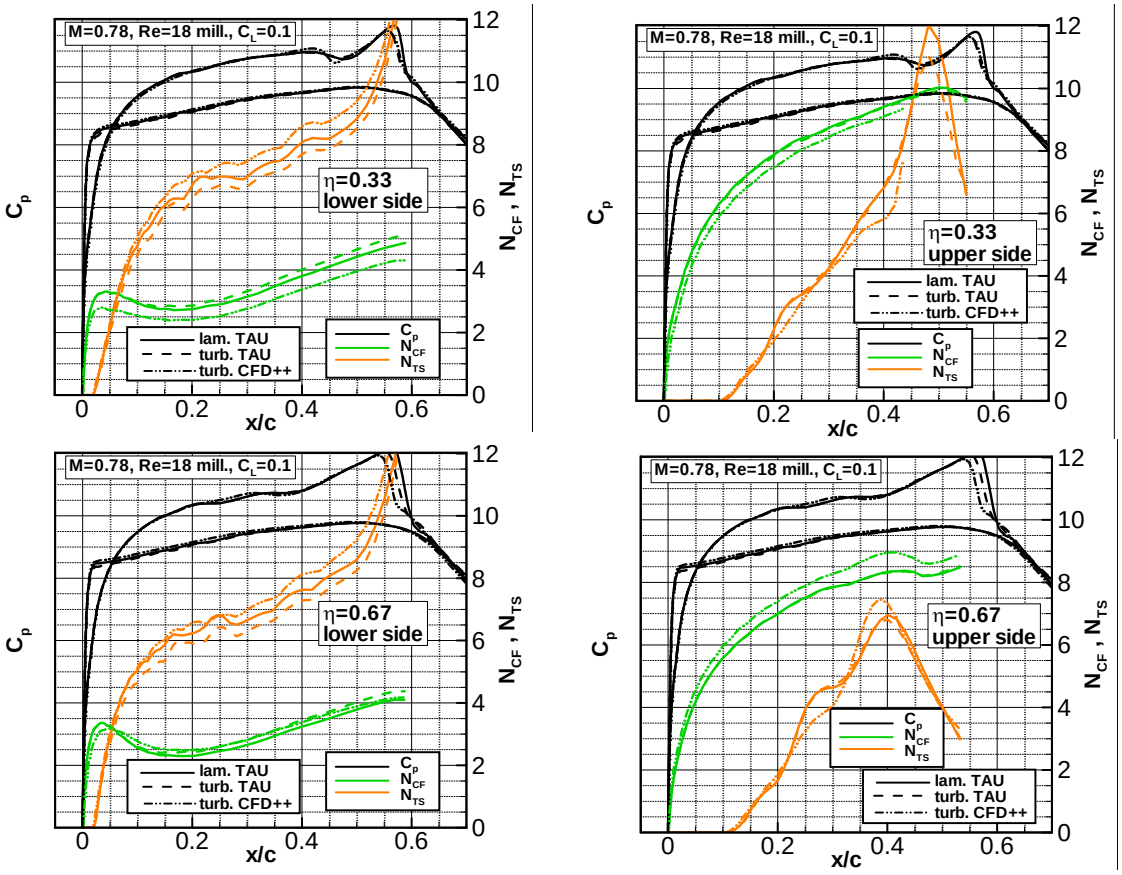

Fig 6. Pressure distributions and stability analysis for RANS solution obtained with CFD++ and TAU.

4.2 Comparison of experimental and numerical results

Seven cases from the first and second ETW Telfona Pathfinder test campaigns are selected to perform stability analysis. Stability analysis is based on ETW, TAU-RANS and CFD++ pressure distributions. Flow conditions for these cases are given in table 1. The comparison of stability analysis for numerical and experimental pressure distributions is given in Fig. 7-14. Data are compared at two sections with span=0.33 and 0.67 for upper and lower surface. For the experimental results the figures include data for the corresponding starboard and port wing section. Especially for the N_{CF}-factor

the effective sweep [12] plays an important role. For the experimental cases effective sweep was predicted with sufficient accuracy indicating that the number of pressure taps in the stagnation line area is sufficient dense. Except for cases 2 and 4, the effective sweep angle used for stability analysis was the one obtained by the pre-processing tool PREPCP. For the experimental cases 2 and 4, the effective sweep angle showed some scattering among the sections. To improve the results the average of the experimental values obtained for all 4 sections (2 for port wing and 2 for starboard wing) was taken. Figure 7 compares results with averaged and non-averaged effective sweep for case 4 were differences between obtained port and starboard wing were largest. Note that also the effective sweep angle coming from the CFD solution could have been used.

Case	ETW Test No. (for Cp, for TSP)	CFD method	$Re/10^6$	T_{Tot}[°K]	C_L
1	P081, P085	TAU,CFD++	20^+	175	0.10
2	P086, P087	TAU	20	175	0.21
3	P088, P089	TAU	20	175	0.32
4	P090, P091	TAU	20	175	0.401
5	P092, P093	TAU	20	175	0.498
6	P254, P255	CFD++	10	175	0.46^*, 0.45^{**}
7	P268, P269	CFD++	10	175	0.10

Table 1: Flow conditions for selected cases with M=0.78, ß=0°. *ETW, **RANS. +For case 1 the CFD++ results were obtained at Re=18 mill. But stability analysis was performed at 20 mill.

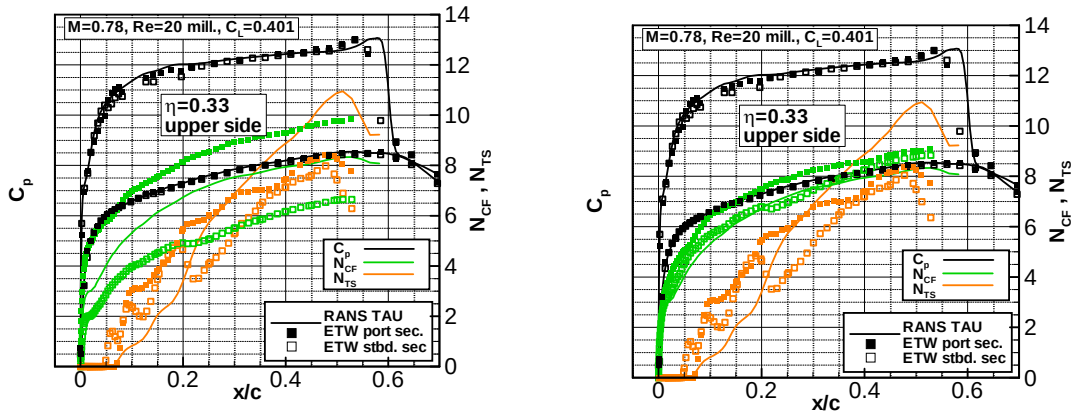

Figure 7. Comparison of experimental and numerical stability analysis results for case 4 upper side. Left side with non averaged and right side with averaged experimental effective sweep.

The comparison of stability analysis for numerical and experimental pressure distributions for cases 1-7 is given in Fig. 8-14.The agreement between N-factors based on numerical and experimental pressure distributions is good, in some cases very good (section η=0.33, lower side, cases 2-4,7). Differences are in some cases larger for N_{TS} (e.g: section η=0.33, upper side, case 5) than for N_{CF}, but it is of the same order of magnitude as the difference between corresponding experimental N_{TS} data from port and starboard wing sections. Since the numerical solution for the pressure distribution is smoother in the nose region, N_{TS}-differences also occur at the nose region (x/c< 0.2). However N_{TS} is small for this region.

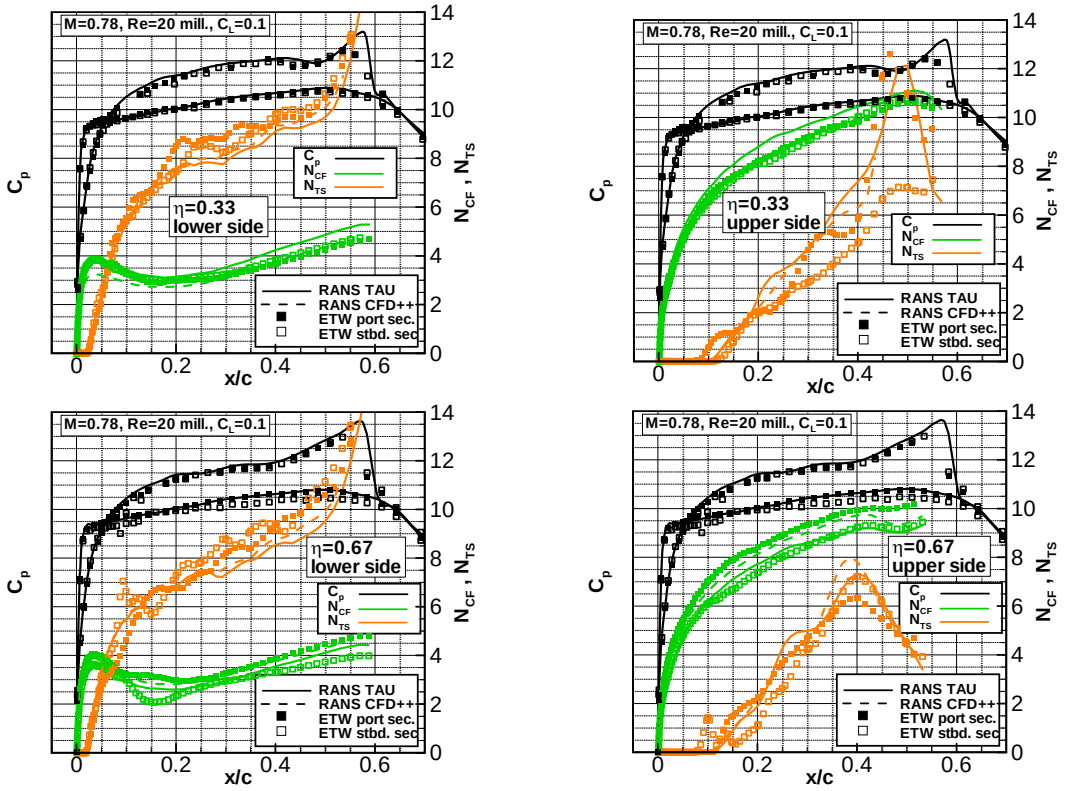

Figure 8. Case 1:ETW and numerical results for pressure distributions and stability analysis. CFD++ results were obtained at Re=18 mill, but stability analysis was performed at 20 mill.

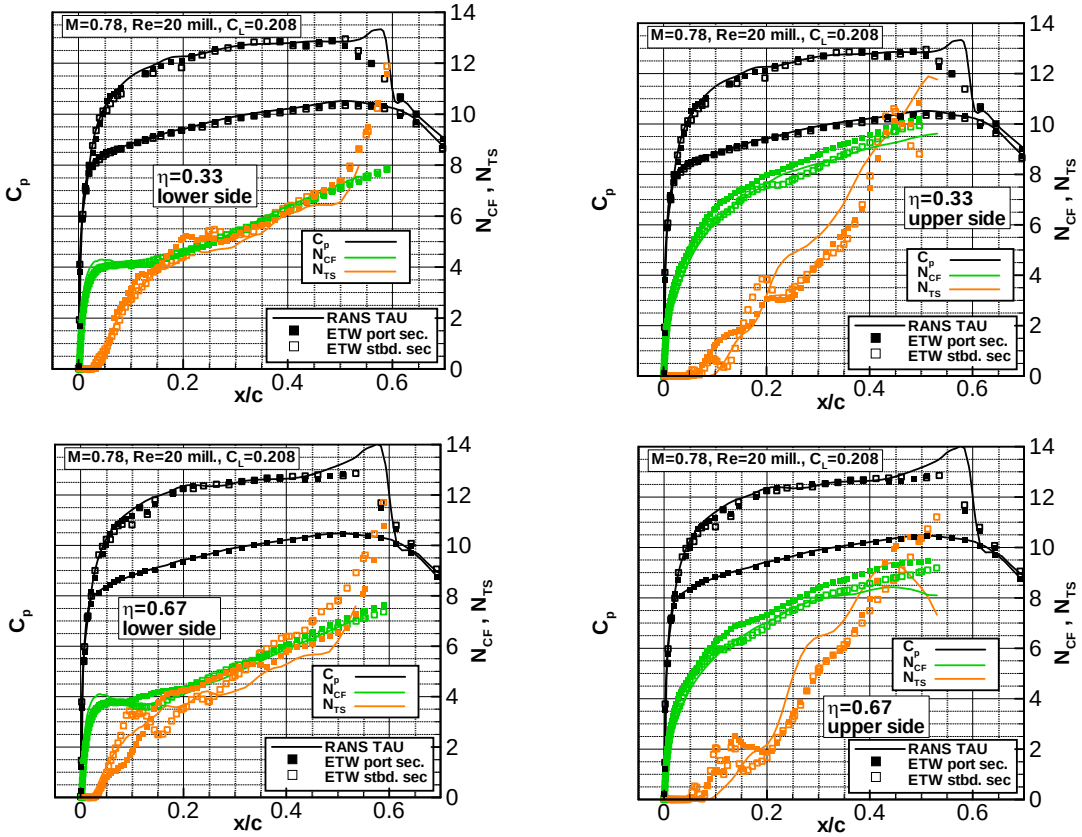

Figure 9. Case 2: ETW and numerical results for pressure distributions and stability analysis.

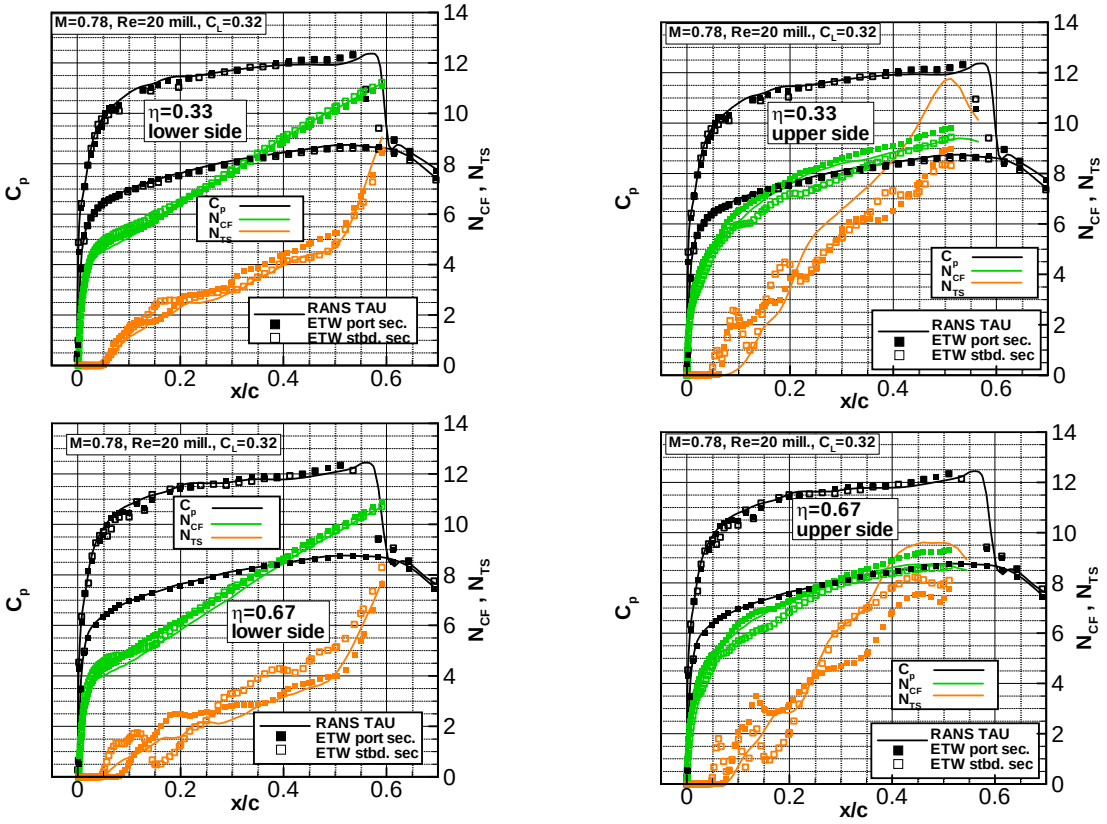

Figure 10: Case 3:ETW and numerical results for pressure distributions and stability analysis.

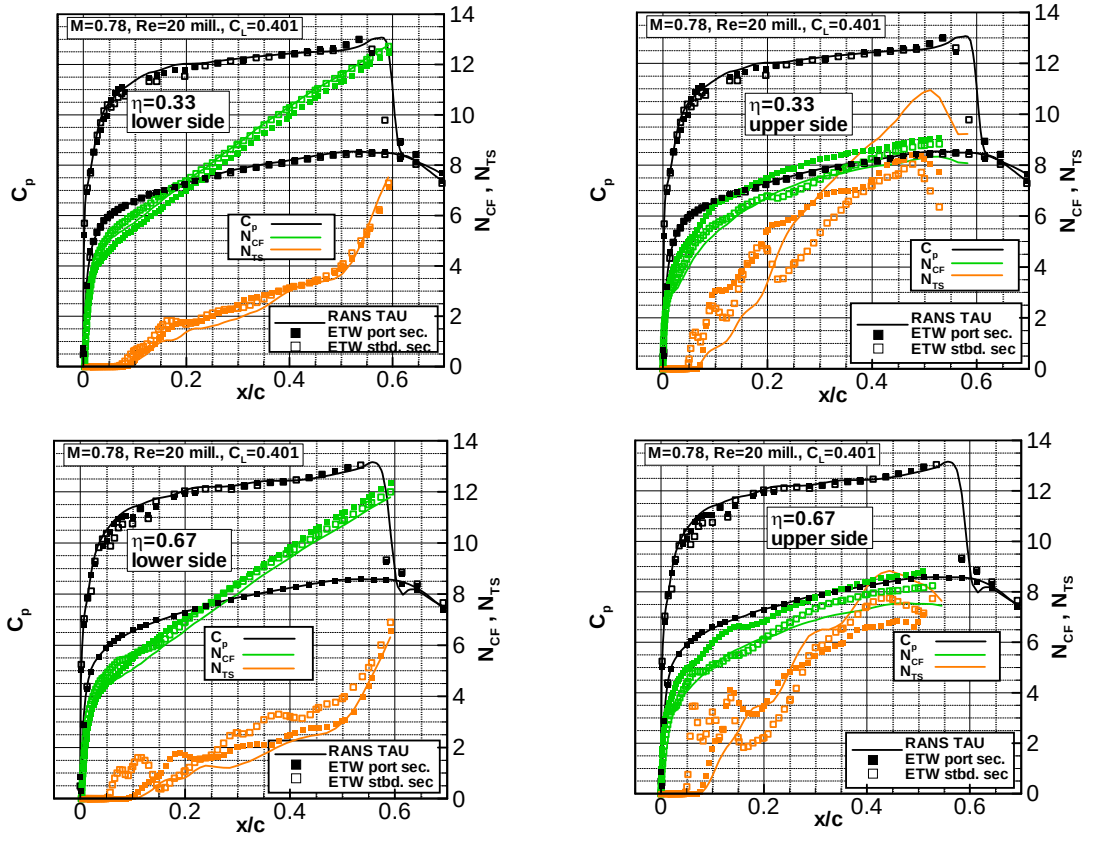

Figure 11: Case 4: ETW and numerical results for pressure distributions and stability analysis.

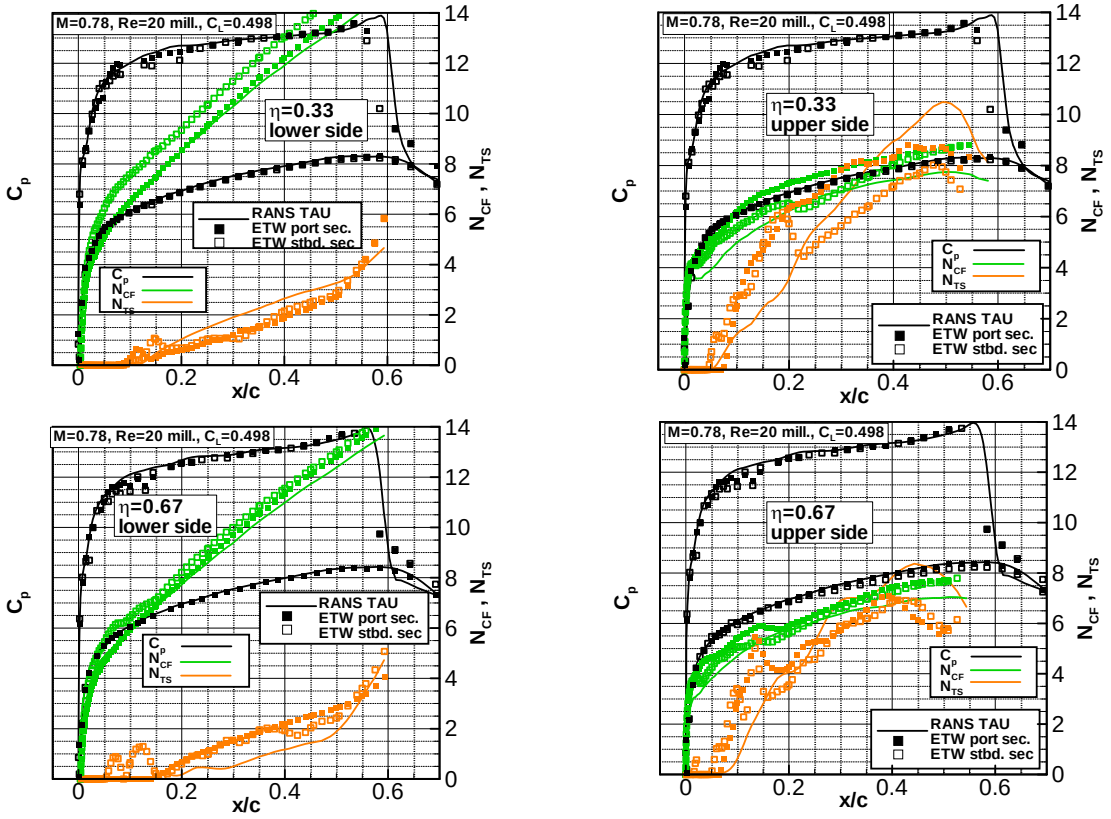

Figure 12 Case 5: ETW and numerical results for pressure distributions and stability analysis.

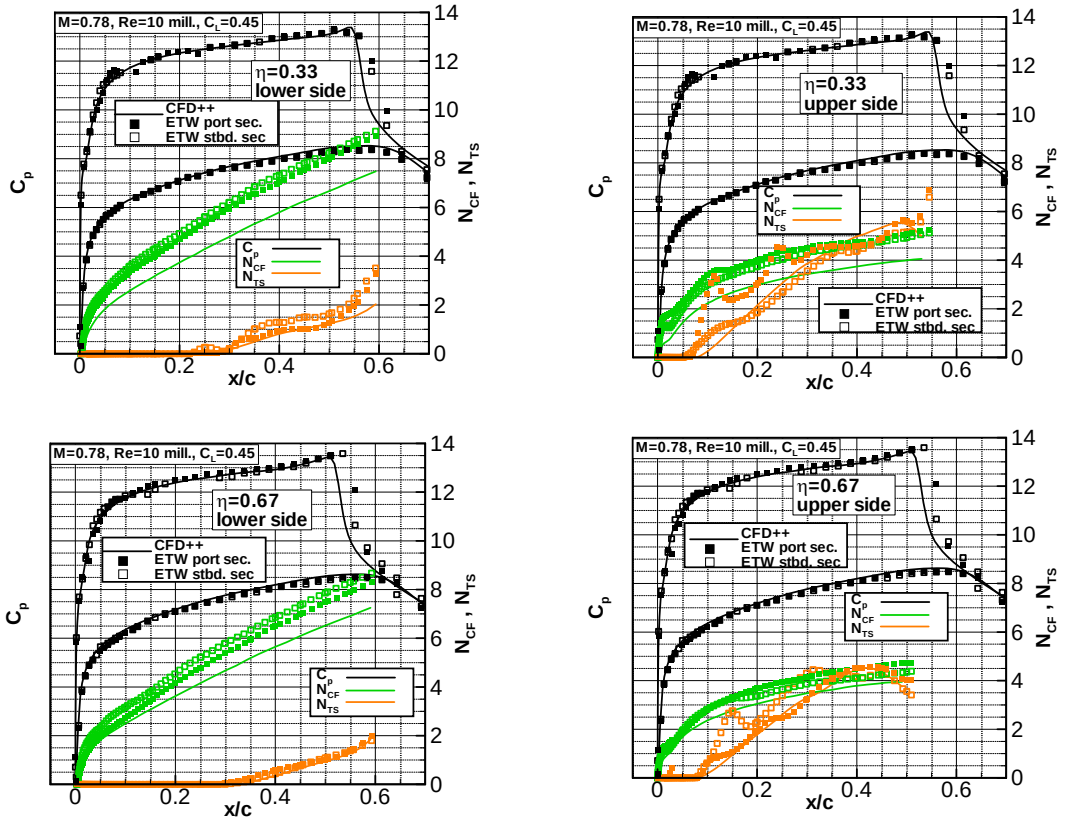

Figure 13. Case 6:ETW and numerical results for pressure distributions and stability analysis.

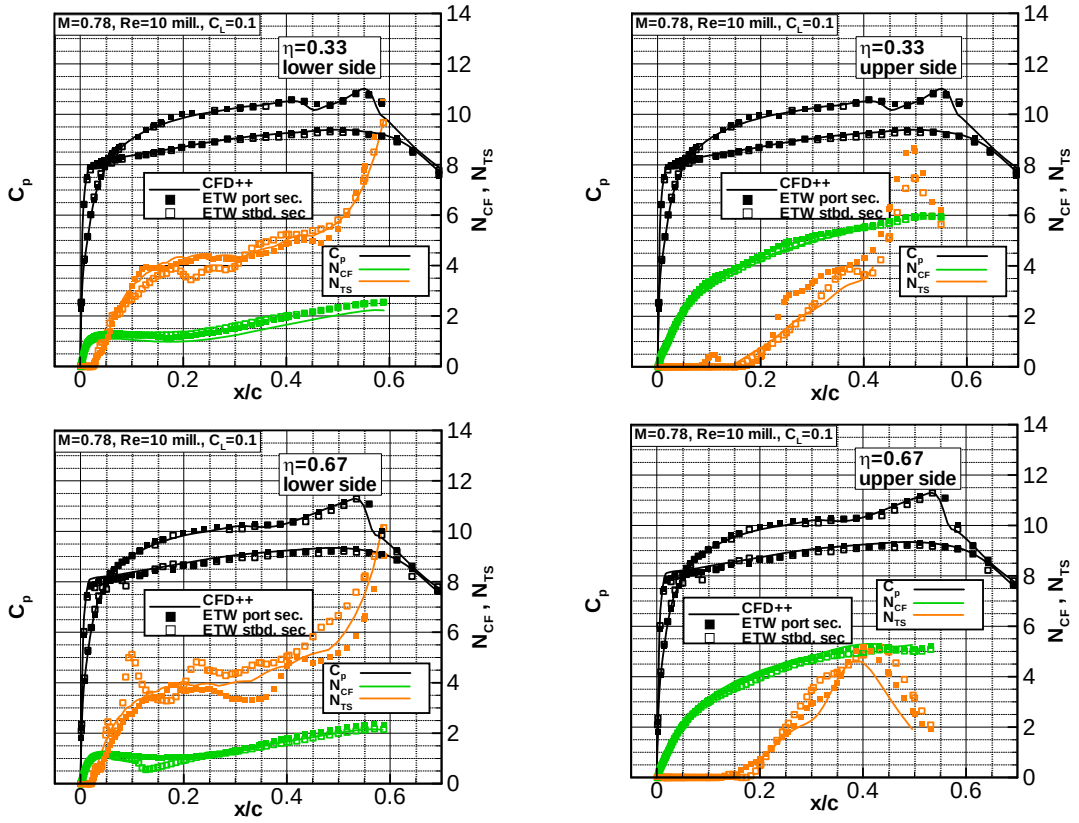

Figure 14. Case 7:ETW and numerical results for pressure distributions and stability analysis.

4.3 Results for ETW Pathfinder Phase III test campaign

TSP data and pressure distributions from test campaigns I and II have been used to obtain transition N-factors [3],[4]. For ETW Phase III, there exists TSP data but no experimental pressure distributions. Therefore to obtain transition N-factors pressure distributions are obtained using CFD solutions.

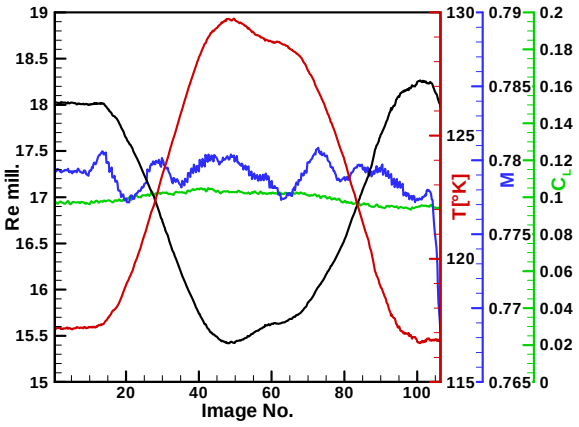

Figure 15. Change of flow conditions for Polar 699.

TSP images exist for the whole step up/step down- process. Within one polar during the temperature step up /step down measurement process, Re number and to a less extent M & C_L change. Accordingly transition changes its position in the corresponding TSP images. Therefore ETW Phase III offers several new cases for correlation. Variation of flow variables is shown in Fig. 15 for Polar 669. In this case for a temperature variation between 117°K to 129°K, Re varies from 15.4 mill. to 18.2 mill. Corresponding TSP images

for maximum and minimum Re numbers for this Polar are given in Fig. 16 for the upper side. They show a TS transition, located at 0.60c for Re=15.4 mill and 0.25-0.30c at Re=18.1 mill.
Fig. 17 shows stability analysis based on TAU-RANS pressure distributions. Solutions are obtained at the Polar 699 minimum and maximum Re number. Flow conditions are: M=0.78, Re=18.1 mill., C_L=0.095, T=116.58 °K and M=0.78, Re=15.4 mill., C_L=0.1032, T=129.74°K.

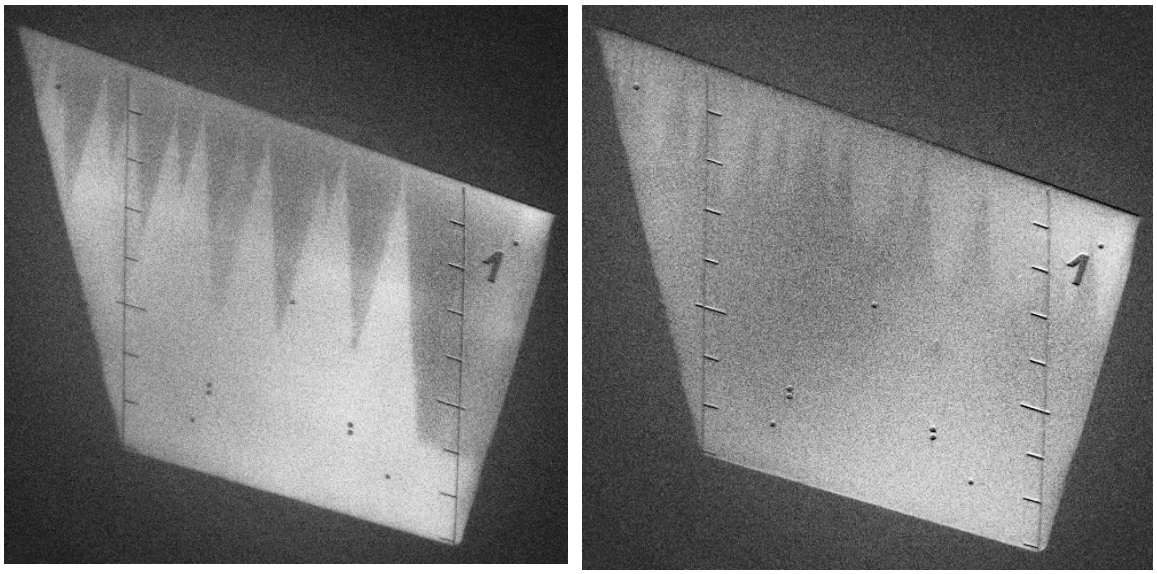

Figure 16. Polar 699: TSP Images for upper wing at maximum (right) and minimum (left) Re number for temperature step up/down measurement.

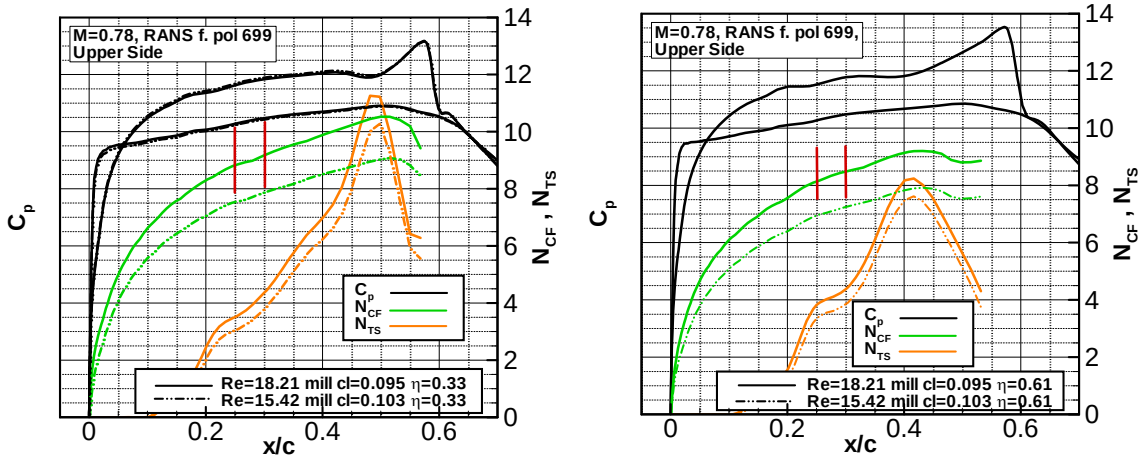

Figure 17. Polar 699: Upper wing stability analysis results for numerical solutions at maximum and minimum Re number for temperature step up/down measurement. The left side shows results at the inboard section and the right side shows results for the outboard section. Red lines correlate transition position from the TSP images for the maximum Re number case.

The TSP images indicate that for minimum Re number, transition at the outboard section occurs at 60% (pressure minimum). For maximum Re-number the CF transition at 0.25c to 0.30c correlates to an N_{CF} value varying between 8.8 and 9.2 for the inboard section and N_{CF} value varying between 8.2 and 8.5 for the outboard section. The results obtained with CFD ++ and TAU for the flow condition M=0.78, Re=18.1 mill. and C_L=0.1 which have been compared in Fig. 6 have flow conditions close to the maximum

Reynolds case from Polar 699. In the region of transition indicated by the TSP methods both numerical methods differ in N_{CF} and N_{TS} by a value $\Delta N_x \approx 0.5$ (see Fig. 6).
Fig. 18 shows stability analysis for M=0.78, Re=10 mill. and C_L=0.45 and a corresponding TSP image from Polar 794. Transition occurs at the shock.

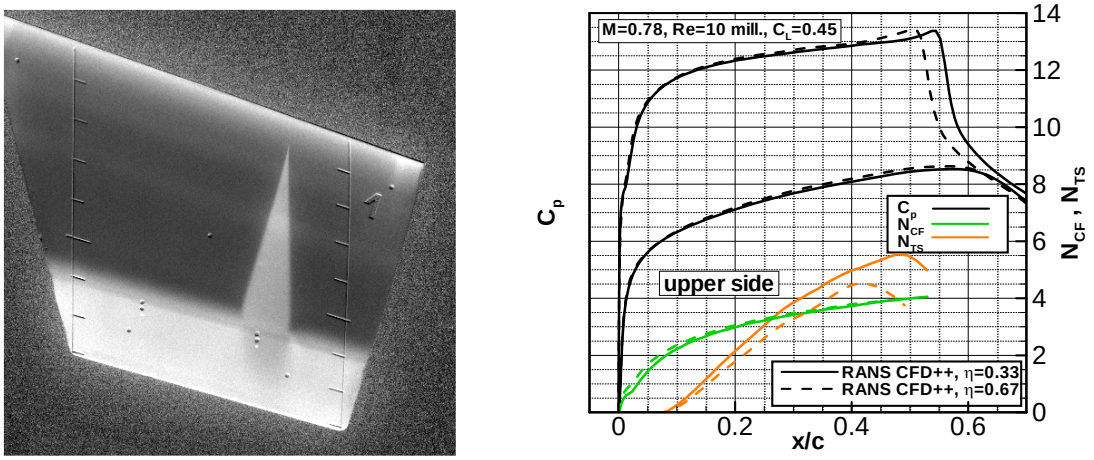

Figure 18. TSP image and stability analysis for Polar 794.

Another useful example for correlation is given in Fig. 19 which shows TSP images indicating the evolution of CF dominated transition at the lower side for C_L=0.45 as function of Re-number.

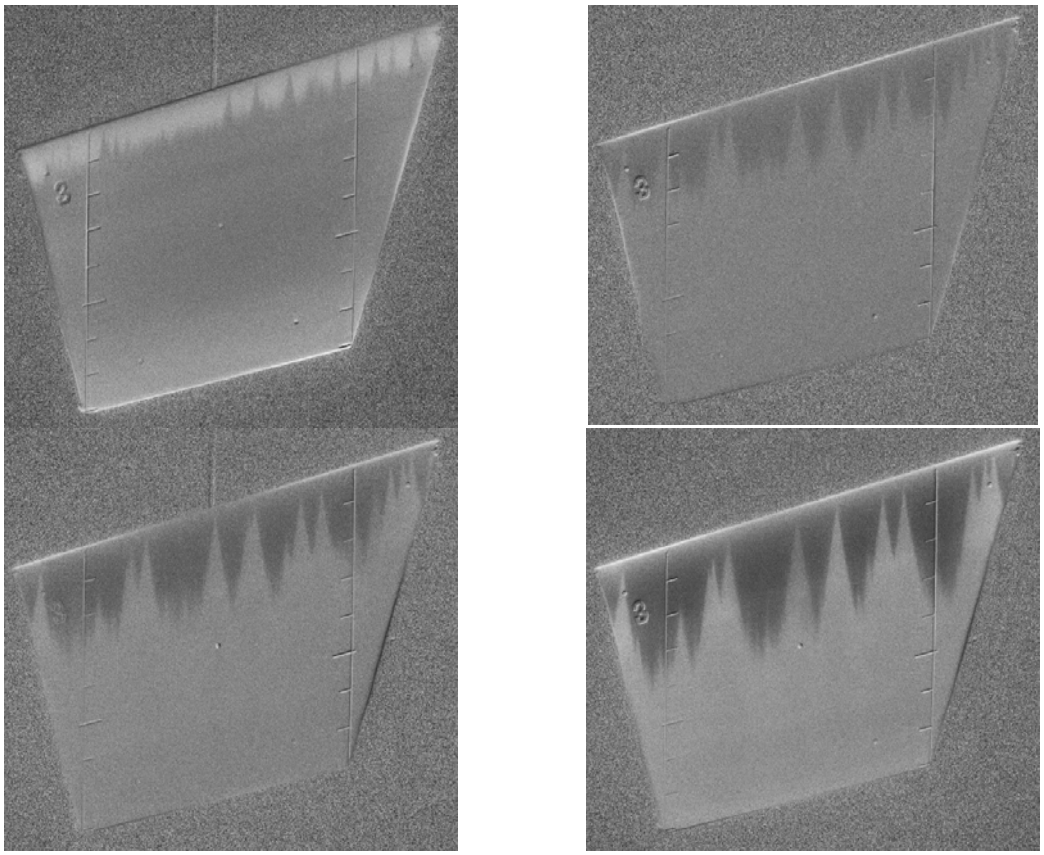

Figure 19. Selected TSP images for Polar 697 & 769 with M=0.78, CL close to 0.45. TSP images: Re=23.0 mill (upper left Pol. 769), Re=16.8 mill. (upper right, Pol. 697), Re=16.0 mill (lower left, Pol. 697), Re=15.3mill (lower right, Pol. 697).

Corresponding CFD solutions are given in Fig.20. The correlated N_{CF} are: 9 to 10 for the Re=23 million case, 7.5 to 8.5 for the Re=16.0 million case and 8.5 to 9.5 for the Re=15.3 mill. case. All CFD solutions were obtained using as wall temperature the adiabatic temperature and this was also assumed for stability analysis. However, the wall temperature may also have an influence.

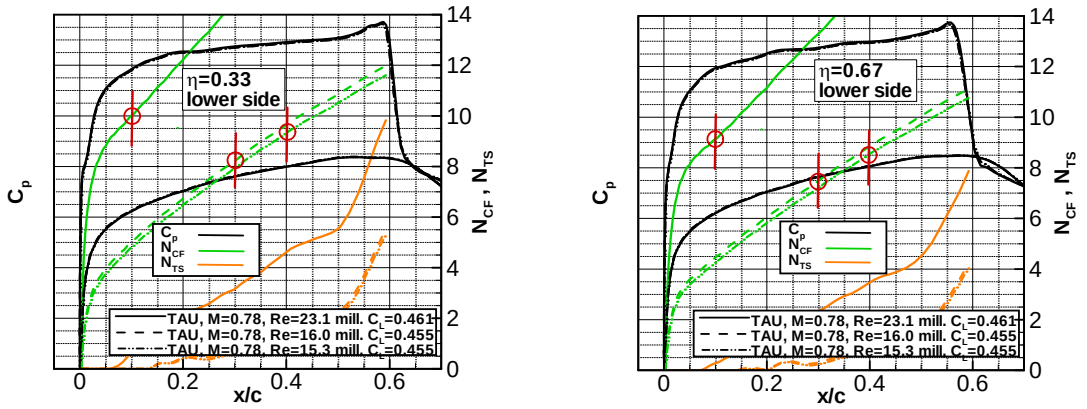

Figure 20. Lower wing stability analysis results for numerical solutions corresponding to TSP images from Figure 19. Red lines correlate transition position from the TSP images

Polar 787:
Re. No. 18 million
Mach 0.78
C_L 0.1
T_{tot} 117

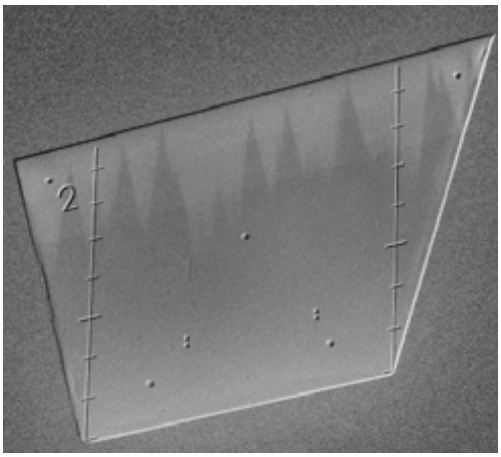

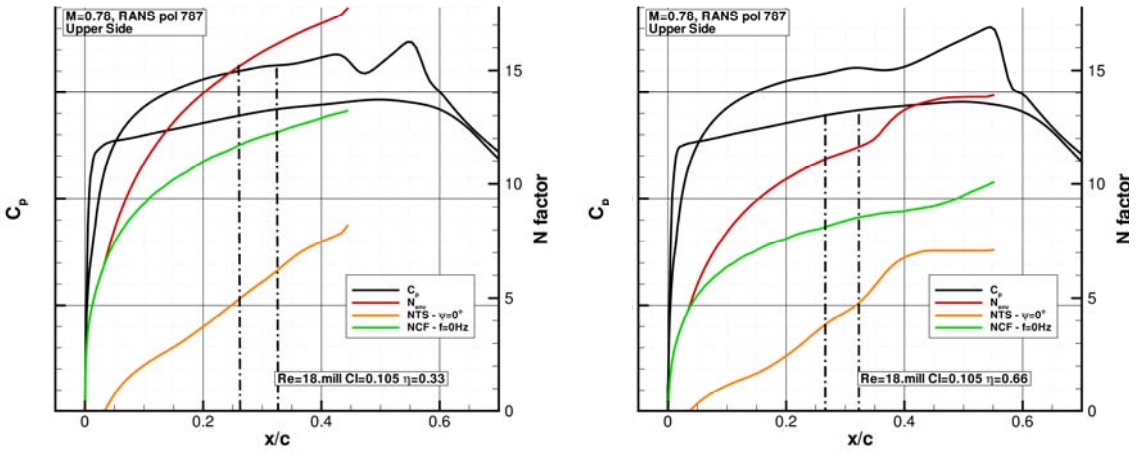

Fig. 21 Polar 787: TSP Image (upper right) and lower wing stability analysis results (lower figures) based on elsA [9] pressure distribution. Dashed lines indicate transition position in the TSP images. The lower left side shows results at the inboard section and the lower right side shows results for the outboard section.

Figures 21 and 22 illustrate the correlation between a TSP image with the numerical analysis of the corresponding CFD results obtained using elsA [9] solver in RANS model for two test cases, respectively 787 and 769. These two cases differ in terms of Reynolds number (Re=18. million for 787 and 23 million for 769) and lift conditions (Cl=0.105 for 787 and 0.48 for 769).
For the 787 case, we observe that the experimental transition (at around 30% of local chord) occurs for computed critical envelope N factors between 12 and 15, whether the outboard or the inboard is considered.

Polar 769:
Re. No. 23 million
Mach 0.78
C_L 0.45
T_{tot} 117

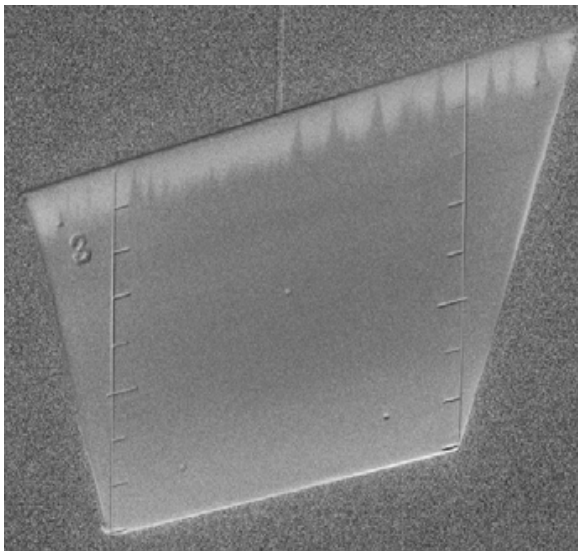

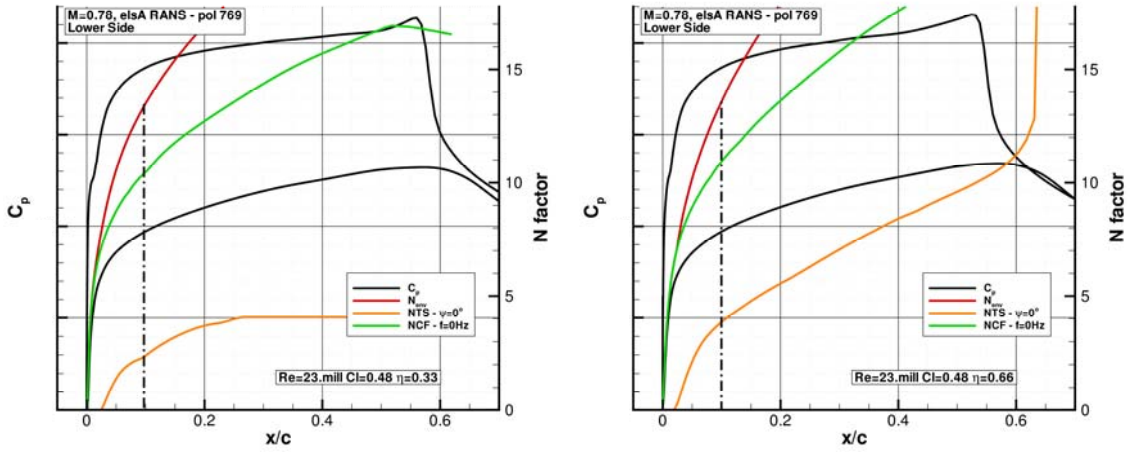

Fig. 22 Polar 769: TSP Image (upper right) and lower wing stability analysis results (lower figures) based on elsA [9] pressure distribution. Dashed lines indicate transition position in the TSP images. The lower left side shows results at the inboard section and the lower right side shows results for the outboard section.

The same range of critical compressible envelope N factor is found when analysing 769 case, for which transition occurs closer to the leading edge (at around 10% of local chord). In both cases transition occurs mainly due to crossflow instabilities triggering. The critical compressible N_{CF0} (0 standing for the 0 frequency mode) factor reaches values around 10 when the N_{TS} remains lower than 5 in the transition region. A good

agreement is observed with the correlations obtained using the DLR/Airbus stability analysis approach.

The evaluation of ETW Phase III cases is still in progress. There are several other interesting cases to be considered.

5 CONCLUSIONS

After test Navier-Stokes mean flow numerical solutions were obtained for the Telfona Pathfinder model using the, CFD++, DLR-TAU and elsA solvers. The Telfona Pathfinder model was designed, analyzed numerically, constructed and tested with the aim to obtain the capability of laminar flow testing of the ETW. The ETW tests provided pressure distribution data and transition position obtained from images using the Cryogenic Temperature Sensitive Paint Method. Stability analysis results were obtained using the N_{TS}/N_{CF} local incompressible stability analysis method LILO. The numerical pressure distributions results, verified the Pathfinder design requirement, that the spanwise variation of pressure distribution is very small, even at off design conditions. This allows the use of stability analysis based on numerical or experimental pressure distributions from constant span sections. It is also shown, that the Pathfinder pressure distribution is not sensitive to the use of turbulence models and either fixing transition or not. For comparison between numerical and experimental results, 7 cases from ETW Pathfinder test campaigns I and II were selected. The stability analysis based on ETW and CFD pressure distributions for these test cases shows good, in some cases very good agreement. Therefore CFD pressure distributions can be used to complement the analysis of the ETW test cases. Especially for the third Pathfinder test campaign this is very useful since no experimental pressure distributions exist. TSP images from ETW Phase III provided several cases where transition position can be used to obtain the transition N-factor. First stability analysis results based on CFD-RANS solutions are presented for selected ETW phase III cases. The analysis of ETW Pathfinder results, using complementary numerical and experimental results is still in progress. It will include the ETW Phase III cases, but will consider also ETW Phase I and II cases in order to improve and complement the determination of the transition N-factors.

AKNOWLEDGEMENT

The work presented in this paper was part of the research project TELFONA, performed under contract No. AST4-CT-2005-516109, financed by the European Union. Thanks to Karl Heinz Horstmann (DLR) and Jean Perraud (ONERA) for useful discussion and advice within this work and to Jürgen Quest (ETW) for providing special required additional post-test data relevant for this work.

REFERENCES

[1] G. Schrauf, K.H. Horstmann and T. Streit, The Telfona Pathfinder Wing for the Calibration of the ETW Wind Tunnel. In Proceedings of the *1st CEAS European Air and Space Conference*, 10-13 September, Berlin, (2007)

[2] U. Fey, Y. Egami, and R.H. Engler, "High Reynolds number transition detection by means of Temperature Sensitive Paint, *AIAA Paper 2006-0514,* (2006).

[3] J. Perraud, J. Archambaud, G. Schrauf, R. Donelli, A. Hanifi, T. Streit, S. Hein, U. Fey, Y. Egami, Transonic High Reynolds Number Transition Experiments in the ETW Cryogenic Wind Tunnel. *AIAA Paper 2010-1300, 48th AIAA Aerospace Sciences Meeting,* 04.-07. Jan. 2010, Orlando, Fl., USA, (2010)

[4]J. Perraud, Itham Salah El Din, G. Schrauf, A. Hanifi, R. Donelli, S. Hein, U. Fey, Y. Egami, T. Streit**.** High Reynolds Number Transition Experiments in the ETW Test Facility with the Pathfinder Model .To appear in: *Proccedings of the V European Conference on Computational Fluid Dynamics,* ECCOMAS CFD 2010 , Lisbon, Portugal (2010)

[5] G. Schrauf, K.H. Horstmann, T. Streit, J. Perraud, and R. Donelli, "The Telfona Pathfinder Wing for the Calibration of the ETW Wind Tunnel" KATnet II *Conference on Key Aerodynamic Technologies*, 12-14 May, Bremen, (2009)

[6] N. Kroll, J.K. Fassbender [Hrsg.]: MEGAFLOW – Numerical Flow Simulation for Aircraft Design, *Notes on Numerical Fluid Mechanics and Multidisciplinary Design (NNFM), 89, Springer Verlag*, Closing Preparation DLR Project MEGAFLOW, 2002 Braunschweig (2002)

[7] O. Peroomian and S. Chakravarthy "A 'Grid-Transparent' Methodology for CFD," In *AIAA Paper No. 97-0724*, Reno (1997).

[8] G. Schrauf "LILO 2.1 – Users "Guide and Tutorial", GSSC Technical Report, July (2006)

[9] M. Gazaix, A. Jollès, M. Lazareff, The elsA Object-Oriented Computational Tool for Industrial Applications. 23rd Congressof ICAS, Toronto (Canada), September (2002).

[10] G. Casalis, D. Arnal ELFIN II, Subtask 2.3: Data Base Method. Development and Validation of the Simplified Method for Pure Crossflow Instability at Low Speed ELFIN Technical Report Nb145, 1996

[11] F: Laburthe., Problème de stabilité linéaire et prévision de la transition dans des configurations tridimensionnelles, incompressibles et compressibles", *Thèse de Doctorat Sup'Aéro,* Toulouse, Dec. (1992)

[12] G. Redecker ,G. Wichmann, , Forward Sweep - a Favourable Concept for Laminar Flow. In Journal of Aircraft, Vol. 28, No. 2, pp. 97-103, (1991)